# Galloping Vibration Monitoring of Overhead Transmission Lines by Chirped FBG Array

Qizhong YAN[1,2,4,6], Ciming ZHOU[1*], Xuebin FENG[5], Chi DENG[6], Wenyu HU[6], and Yimin XU[1,3]

[1]*National Engineering Laboratory for Fiber Optic Sensor Technology, Wuhan University of Technology, Wuhan 430070, China*

[2]*School of Information Engineering, Wuhan University of Technology, Wuhan 430070, China*

[3]*School of Safety Science and Emergency Management, Wuhan University of Technology, Wuhan 430070, China*

[4]*Wuhan WUTOS Co., Ltd., Wuhan 430223, China*

[5]*China Electric Power Research Institute, Beijing 100192, China*

[6]*Wuhan FLOES Co., Ltd., Wuhan 430223, China*

[*]Corresponding author: Ciming ZHOU E-mail: zcm@whut.edu.cn

**Abstract:** A distributed online fiber sensing system based on the phase-sensitive optical time domain reflectometer (Φ-OTDR) enhanced by the drawing tower fiber Bragg grating (FBG) array is presented and investigated experimentally for monitoring the galloping of overhead transmission lines. The chirped FBG array enhanced Φ-OTDR sensing system can be used to measure the galloping behavior of the overhead transmission lines (optical phase conductor or optical power ground wire), which are helpful for monitoring the frequency response characteristics of the ice-induced galloping, evaluating the motion tendencies of these cables, and avoiding the risk of flashover during galloping. The feasibility of the proposed online monitoring system is demonstrated through a series of experiments at the Special Optical Fiber Cable Laboratory of State Grid Corporation of China (Beijing, China). Results show that the proposed system is effective and reliable for the monitoring of galloping shape and characteristic frequency, which can predict the trend of destructive vibration behavior and avoid the occurrence of cable breaking and tower toppling accidents, and these features are essential for the safety operation in smart grids.

**Keywords:** Distributed vibration sensing; FBG array; galloping monitoring; overhead transmission lines

Citation: Qizhong YAN, Ciming ZHOU, Xuebin FENG, Chi DENG, Wenyu HU, and Yimin XU, "Galloping Vibration Monitoring of Overhead Transmission Lines by Chirped FBG Array," *Photonic Sensors*, 2022, 12(3): 220310.

Open Science Identity (OSID)

## 1. Introduction

Optical fiber composite overhead ground wire (OPGW), as the most widely used type of overhead transmission line, includes aerial fiber cable and ground wire. It has double functions of lightning protection and communication. OPGW plays an important role in relay protection, information communication, and power dispatch [1]. Overhead transmission lines are an important part of power

Received: 21 October 2021 / Revised: 6 December 2021

DOI: 10.1007/s13320-021-0651-4
Article type: Regular

grids within the power utility industry, and reliable internal communications are vital to ensure protection and control of the power system, which easily suffers from the impact of complex weather conditions. In addition, galloping is always expected to occur during the service life [2, 3]. Transmission line galloping is wind-induced vibration of single and bundle overhead conductors with low frequency (typically 0.1 Hz to 3 Hz) and large amplitude (approximately 5 times to 300 times of the power transmission line diameter), and it usually occurs in a specific environment with strong winds and transmission line icing and lasts for several hours [4]. Galloping may reduce air gaps between conductors, occasionally causing communication failure, flashovers, and repeated power supply interruptions, which are harmful for power grids. Health monitoring of overhead transmission lines plays a vital role for smart grid construction. Fast and accurate measurement of vibration frequency and movement amplitude along the transmission lines can provide reliable tension information for decision-making, quick response for emergencies, and extreme weather conditions. It also provides advance warning of the possibility of dangerous tensile force variation situation, such as damper performance deterioration, forecasting of transmission line icing, and other possible abnormal motion state, thereby reducing unnecessary manual intervention. Traditional monitoring methods include electric acceleration sensor, video image detection, radar detection, and some wireless detection technology methods. All these technologies have many problems, such as difficulty in obtaining power on site, single point separation measurement, and extremely expensive for large-scale applications, which do not fulfill the application requirements of smart grids and cannot achieve successful market application promotion [5–7].

Currently, the fiber optic sensing technology is widely adopted for health monitoring and evaluation of overhead transmission lines in power grids because of its immunity to electromagnetic interference, capabilities of multiplexing and distributed sensing, and tolerance to harsh environments [8]. Two main fiber optic sensing technologies applied in transmission lines are the fiber Bragg grating (FBG) sensing and distributed sensing technologies. FBG sensors are stable, cheap, and portable demodulation system. On the contrary, the distributed sensing technology requires a highly demanding light source and a demodulator, but it can utilize the fiber in optical phase conductor (OPPC)/OPGW directly without extra packaging and installation processes. Any point information along the OPPC/OPGW can be measured by distributed sensing technologies. Fiber optic sensing-based early fault monitoring systems in smart grids are accelerated by the extensive applications of OPPC and OPGW [9]. A researcher in Norway investigated the transmission line aeolian vibration monitoring via the surface-mounted Bragg grating (FBG) sensors in 2000 [10]. A distributed online fiber sensing system based on the combination of Brillouin optical time domain reflectometry (BOTDR) and FBGs is proposed for icing monitoring [11]. A detection system composed of FBG tension sensors, installed between an insulator string and a power tower, is designed to detect the dynamic tension and galloping of overhead transmission lines [12]. Recently, the galloping frequency of the transmission lines can be monitored by phase-sensitive optical time domain reflectometer (Φ-OTDR), which is one of the most popular fiber optic sensing technologies for vibration and sound measurement, and some preliminary results emphasize a collaboration of the FBG and Φ-OTDR in terms of confirming the galloping event and evaluating the tower safety [13]. More comprehensive and reliable information on power grids can be obtained by combining different optic sensing technologies and applying them collaboratively in power grids. This approach is the

development trend of the future and an excellent opportunity of the fiber optic sensing technology in smart power grids.

With the development of an on-line FBG writing technique, the multiplexing capacity of an FBG array can be significantly increased using wavelength-division multiplexing (WDM), time-division multiplexing (TDM), or the combination of the two techniques [14, 15]. Moreover, the Φ-OTDR assisted with the ultra-weak FBG array has been proposed with pico-strain dynamic resolution and improved the response bandwidth by the multiple input and multiple output (MIMO) coding technology [16]. An auxiliary interferometer was employed for reducing the effect of the laser phase noise to solve the noise problem at the low frequency range [17]. Liu *et al.* [18] demonstrated a high precision detection system with ultra-low frequency sensing resolution of sub-nε resolution in mHz frequency range. As the Φ-OTDR has demonstrated efficient seismic acquisition ability in seismology application such as natural hazard prediction and crust exploration, and the ultra-weak FBG array sensor technology can realize wide-band, low-noise or multi-parameter measurement, there are no doubts that the ultra-weak FBG array sensing technology will play a more important role in the field of subway tunnel structure safety monitoring and geoscience research [19–23].

In this paper, a distributed online fiber sensing system based on the novel chirped FBG array, which is prepared by the drawing tower technology, is firstly presented, and investigated experimentally for the online galloping monitoring of overhead transmission lines. The Φ-OTDR enhanced by the chirped FBG array has better detection sensitivity and signal reduction ability than the commonly used Φ-OTDR, which adopts single-mode optical communication fiber. A distributed vibration fiber sensing system (DVS) is used to measure the galloping motion characteristics of overhead transmission lines. Some theoretical and experimental results are provided to verify the feasibility of the proposed system. Some key problems or attentions are discussed to analyze the potential applications for the distributed online fiber sensing system on high voltage overhead transmission lines.

## 2. Operation principle

Ordinary Φ-OTDR uses common randomly distributed Rayleigh scattering light (RBS) with random fluctuation for detection. The signal detection sensitivity exhibits random fluctuation and nonuniformity, and there is also polarization fading problem. As unable to accurately signal calibration, it is mainly used for qualitative analysis. In practical application, it mainly extracts spectrum information of the vibration signal, and the limitation of random amplitude response restricts the deep application of this technology [24–26].

Figure 1 depicts the large-capacity ultra-weak fiber Bragg gratings array (UWFBGs), which is divided into $N$ fiber sections (FSs) of length $L$, and each FS contains paired UWFBGs with chirped characteristics. The DVS technology is an optical time domain reflection system with phase recovery capability designed by utilizing the local reflection units formed between the paired UWFBGs. Identical UWFBGs are inscribed into the sensing fiber with constant interval by using the online writing technology to obtain distributed information along the sensing fiber and reconstruct vibration information. These UWFBGs act as artificial scattering mirrors with stable reflectivity, controllable position, more uniform, and strong reflection lights. Whereas, the phase difference from two given sections has a definite linear relationship with the fiber length changes between the two sections. Therefore, by measuring the phase difference variation between these paired UWFBGs, the dynamic strain induced by external vibration can be quantified [27].

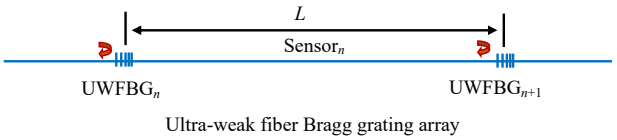


Fig. 1 Sensing part based on FBG array.

Due to photo-elastic effect, the small scaling exerted on the sensing fiber leads to fiber length variation by $\Delta L$ and causes the phase difference between the reflection lights from adjacent UWFBGs to change by $\Delta\varphi$. The relationship between $\Delta L$ and $\Delta\varphi$ can be written as

$$\Delta\varphi = \frac{4\pi n}{\lambda} \cdot \Delta L \tag{1}$$

where $n$ is the effective refractive index of the fiber and $\lambda$ is the wavelength of pulsed detection light source. The phase difference change, $\Delta\varphi$, shows a linear relationship with fiber length variation $\Delta L$. Hence, it is clear that $\Delta L$ can be obtained by demodulating the phase difference change $\Delta\varphi$. Any disturbance event occurring within two UWFBGs can be monitored by demodulating the phase difference change $\Delta\varphi$, ensuring the fully distributed sensing capability of the proposed scheme.

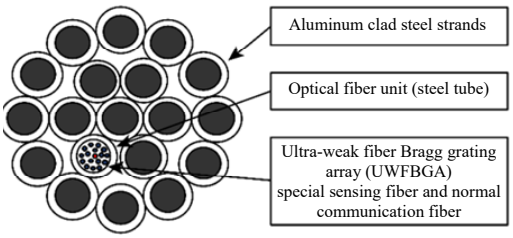


Fig. 2 Cross section of OPGW cable.

A typical OPGW structure is selected in the present study. As shown in Fig. 2, the main structure of the OPGW cable with the special FBG array inside the optical unit is aluminum clad steel strands. We use only one optical unit to place the fiber. The FBG array sensing fiber and the communication fibers are in the same optical unit, which is protected by a capillary stainless-steel tube. The central position of the optical cable structure used in this research is aluminum clad steel stranded wire, which is mainly used to increase the tensile resistance of the optical cable. The optical unit is placed in the second layer structure, and the position of the sensing fiber is slightly deviated from the central position of the optical cable.

As shown in Fig. 3, the sensing fiber is distributed in a spiral shape due to the residual length of the optical fiber in OPGW cable. In general, the longitudinal strain of the OPGW cable cannot be directly transmitted to the sensing fiber. However, the optical fiber and aluminum clad steel wire are composite, but when they move together, both have the same acceleration, thus through this way, we can sense the motion of the aluminum clad steel stranded wires. Then the relationship between the phase difference information measured by the sensing fiber and the vibration amplitude of the optical cable is deduced as follows.

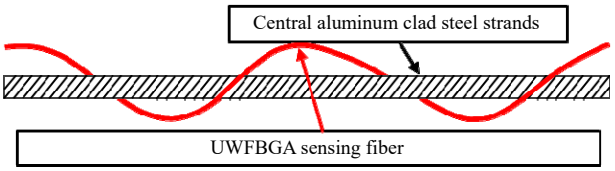


Fig. 3 Physical model of OPGW cable with excess fiber length.

The acceleration of the sensing fiber with a mass of $M$ is the same as that of the whole OPGW cable. Meanwhile, since the optical fiber is spiral, assuming that its elastic coefficient is $K$ and its shape variable is $\Delta L$, the force on the sensing fiber is as follows [28]:

$$F = M \cdot a = K \cdot \Delta L . \tag{2}$$

where $M$ is the mass of the sensing fiber and $a$ is the acceleration of the sensing fiber. When the vibration displacement of the optical cable is $S$, the second derivative of displacement is the acceleration, which is the same as that of the sensing fiber. Equation (1) is substituted into (2) to obtain

$$S \propto G \cdot \Delta\varphi^2 \tag{3}$$

where $G = \left( \frac{K}{M} \cdot \frac{\lambda}{4\pi n} \right)^2$, which is a constant factor. The vibration amplitude of the OPGW cable is proportional to the square of the measured phase

change by the DVS demodulation equipment.

## 3. Experiment and results

The main technical indicators of the DVS used in this experiment are shown in Table 1. We use a 3 kHz narrow linewidth laser (RIO ORION™ Series) as the laser source, and the phase demodulation technology is based on a 3×3 coupler [15]. The analog circuit of this Φ-OTDR system uses a variety of amplifier parameter settings. The dynamic range refers to the detection ability of broadband signal that can be realized by the signal demodulation system when all the unsaturated amplifier parameters are fully applied.

Table 1 Main technical parameters for UWFBGA Φ-OTDR system.

| Parameter | Unit | Values |
|---|---|---|
| FBG reflectivity | dB | –40 |
| FBG spectrum Bandwidth@3 dB | nm | 2.0 |
| FBG spacing | m | 2 |
| Laser pulse width | ns | 10 |
| Detection distance | km | 10 |
| Sampling rate | kHz | 5 |
| Dynamic range | dB | 90 |
| Noise level | pε/√Hz | 82 |
| Laser wavelength | nm | 1 550.23 |

An OPGW-113 aluminum clad steel wire (Provided by FiberHome Telecommunication Technologies Co., Ltd.) is selected in this experiment. As shown in Fig. 2, it comprises 18 aluminum clad steel strands with a diameter of 3 mm as steel core and one stainless steel tube with a diameter of 2.85 mm as the optical unit. The specification parameters of aluminum clad steel wire are shown in Table 2. The mixing optical unit includes 16-core communication fiber and one-core vibration sensing fiber, and the FBG array's interval is 2 m. The rated tensile force of the OPGW cable is 136 kN.

The feasibility of the proposed DVS online monitoring system is demonstrated through aeolian vibration and galloping movement measurement at the Special Optical Fiber Cable Laboratory of State Grid Corporation of China (Beijing, China) in accordance with the items of C.3.1 and D.3 in the Chinese standard: DL/T 832-2016-Optical fiber composite overhead ground wires.

Table 2 OPGW main performance.

| Parameter | Unit | Values |
|---|---|---|
| Cable diameter | mm | 15 |
| Cable structure | --- | 1/3.0/20AS+5/3.0/20AS+12/3.0/20AS, SUS 1/2.85 |
| Weight | kg/km | 802 |
| RTS | kN | ≥136 |
| Average operating tension | --- | 16%–25% RTS |
| Elastic modulus | GPa | 162 |
| Mixing optical unit | Core | 16+1 (UWFBGA) |
| Fiber redundant length | --- | 2.6‰ |
| Grease filling | --- | 85% |

In accordance with the on-site usage of the OPGW cable, the movement range of the OPGW cable caused by the breeze is in the millimeter order, and the frequency is from 10 Hz to 100 Hz. The experimental device that simulates aeolian vibration under laboratory conditions is shown in Fig. 4, where the OPGW cable is subjected to a pull of 35 kN (Normal 25% rated tensile strength), which can be read out by the force sensor (CASC-BK-1B-100kN) at Point B. The OPGW cable is stimulated by a vibration exciter (STI-DC-1000), as shown in Fig. 5, the amplitude of the exciter is set to 1 mm (smallest vibration amplitude that can be used), and the exciter frequency is swept from 10 Hz to 80 Hz (optimal frequency range for simulating aeolian vibration. The OPGW cable cannot be excited when the driving frequency is below 10 Hz, and the exciter cannot work well when it is set near 80 Hz). The DVS demodulator is close to the side of Point A.

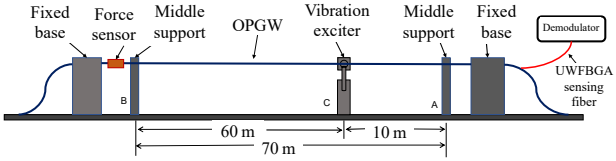


Fig. 4 Experimental device for simulating aeolian vibration.

Fig. 5 Vibration exciter for simulating aeolian vibration.

We choose the location (Point C) near the vibration exciter as the data observation point. The time and frequency domain signals are shown in Fig. 6. The images show the time domain and corresponding spectral map signals detected by vibration frequencies at 10 Hz. Although the sensing fiber is inside the OPGW optical unit and has fiber redundant length of approximately 2.6‰, it can still sense the external vibration signal and accurately measure the excitation signal frequencies. Signal distortion is very low at 10 Hz, as shown in Fig. 6, which is close to standard sine excitation signals. According to the experimental results, the driving frequency obtained by the DVS system is accurate, and it is the same as the frequency of the excitation signal.

In order to verify (3), it is necessary to study the relationship between the OPGW cable vibration amplitude and phase difference signal. For convenience, Point C is selected as the observation point to record the motion amplitude of the OPGW cable, as shown in Fig. 4. The working frequency of the vibration exciter is fixed at 10 Hz, and the moving amplitude of the excitation varies from 0 to 10 mm. The phase difference change information of different excitation amplitudes is obtained through the DVS, as shown in Fig. 7. By parabola fitting, the scaling factor $G$ in (3) can be estimated. The results show that the galloping vibration amplitude of OPGW cable can be detected by measuring the phase difference change, and the experimental results agree with the theoretical expectation.

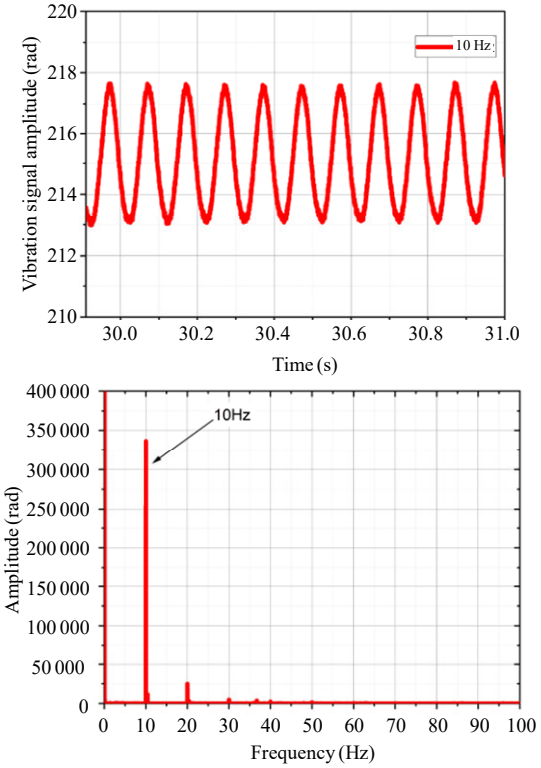


Fig. 6 Vibration signals obtained at 10 Hz exciter frequency settings.

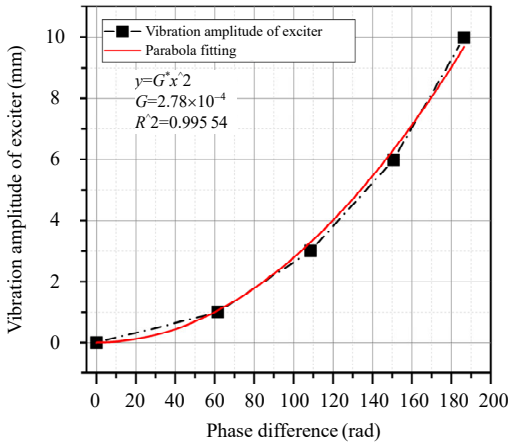


Fig. 7 Relation between the OPGW cable motion amplitude and the phase difference measured by DVS.

When certain conditions are met, the OPGW optical cable shows a standing wave motion state during aeolian vibration [29]. Then, we test the standing wave state response ability, and the correspondence between the OPGW cable motion amplitude and the phase difference measured by

DVS is verified. The output frequency and driving amplitude setting of the vibration exciter are adjusted to better excite the motion of the standing wave form. Thus, the testing OPGW cable shows a visible standing wave motion state. Through testing, when the excitation frequency is tuned to 10 Hz with a vibration amplitude of 10 mm, the OPGW is prone to a clear standing wave form, as shown in Fig. 8. The signal strength near the exciter position C is the strongest, that is, at the length of 10 m. The one-dimensional (1D) curve also clearly shows the phenomenon that the vibration energy attenuates with an increase in the propagation distance. After 70 m, the vibration can continue to propagate beyond the fixed position (Point B), which shows the high sensitivity level of the DVS detection system. As shown in Fig. 8, we measure the distance between standing wave nodes with artificial tape to obtain the wavelength parameters of standing wave. We can clearly observe the nodes and antinodes, and this kind of motion patterns is consistent with the real movement. The number of nodes of the standing waves measured by our DVS is the same as that observed with a high-speed camera.

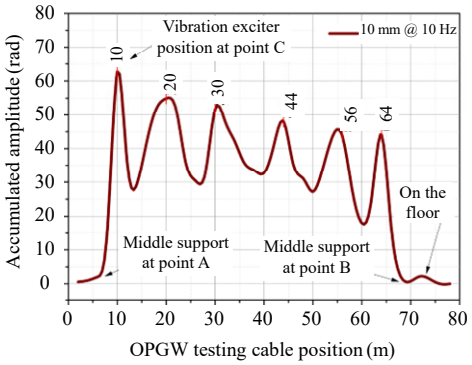


Fig. 8 1D signal of the standing wave.

When the OPGW cable presents a standing wave motion pattern, the amplitude of the optical cable at the node is minimum, and the amplitude at the antinode appears the maximum. The change amplitude of the phase signal obtained by the FBG array sensing cable shows a clear picture in Fig. 8 by marking the peak position of the 1D curve to obtain the wavelength information of the standing wave. According to the data in Fig. 8, the half wavelength of the standing wave is 10.8 m (the peak data are subtracted from the figure one by one to obtain the wavelength of the adjacent standing wave waveform, and the average of the data is obtained). Compared with the 9.8 m value obtained by manual measurement in Fig. 9, that is a measuring method with tape measure, an error of 1 m is obtained. The spatial sampling resolution of the DVS demodulation system is limited by the density distribution of the FBG arrays to 2 m. The difference is mainly due to the under-sampling error caused by insufficient spatial resolution. As it takes a certain amount of time from the initial application of excitation signals to the formation of stable standing waves, data interception starts 20 s after the shaker begins to apply excitation signals in Fig. 10. The waterfall chart over 10 s time along the 80-meter-long OPGW testing cable shows the stable standing wave pattern, and the evident difference between the

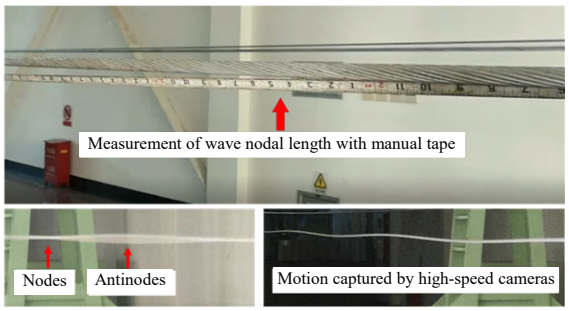


Fig. 9 Screenshot of the video image of standing wave motion pattern.

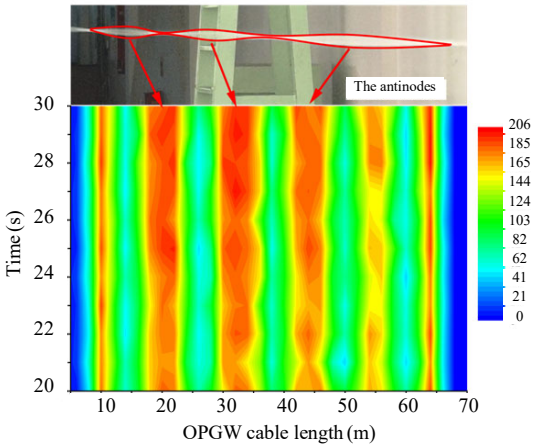


Fig. 10 Envelope of standing wave pattern motion and 2D waterfall signal.

antinodes and nodes is visible to the naked eye. Because the OPGW cable is very long and the width of the room is limited, the camera can only capture three complete nodes and antinodes, which is just a part of the total vibration of OPGW, as shown in Fig. 10. By summing up the phase differential signals at the same location, the nodes and antinodes show a stable high contrast in the two-dimensional (2D) waterfall picture [30]. The red line shows the envelope shape of the standing wave's amplitude of motion, which is taken from a screen shot of a video image.

The simulation test device for realistic large-scale low-frequency galloping behavior is shown in Fig. 11(a). The tension of the OPGW optical cable is set to 3 kN (default tension is 2%RTS), which is convenient for the cable to move in a large amount [17]. The length of the optical cable in the test section from Point A to Point B is 60 m. The cable galloping tester (JP-20-20 kN), shown in Fig. 11(b), is located at Point D, the suspension device is located at point E, and the demodulator is close to Point A. The maximum vibration amplitude of the A-E section of the optical cable exceeds 1 m, which is considered a galloping state, as shown in Fig. 11(c).

The galloping tester can apply excitation signals of different frequencies to the OPGW testing cable. As shown in Fig. 12, the data curve shows the changes in the phase signal along the test cable under the two excitation frequencies of 1.5 Hz and 1.7 Hz. The suspension point is 40 m away from the position A, and the AE section is mainly used in the experiment. The movement amplitude observed with the naked eye is used to judge whether it reaches the galloping state. When the AE section of the OPGW cable dances up and down, the B-E section is in an elliptical motion state, and its swing amplitude is slightly weaker than that of the AE section. E is a suspension point, thus, its vibration amplitude is low. The two ends of the test cable are placed on the floor in a static state, thus, the signal value at the head and tail of the test cable is the smallest. When the excitation signal is 1.7 Hz, the cable's galloping amplitude is the largest, and the AE-segment optical cable's motion amplitude is less than 1 m at 1.5 Hz, that is, it does not enter the largest galloping state.

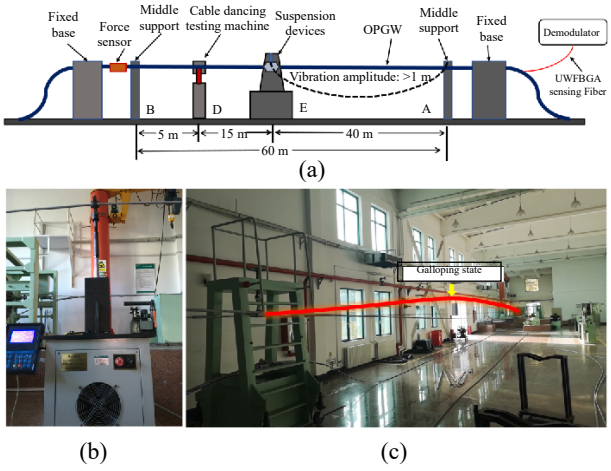


Fig. 11 Experimental device for simulating OPGW cable galloping movement: (a) galloping simulation devices, (b) OPGW cable galloping testing machine, and (c) suspension device and OPGW cable in galloping state.

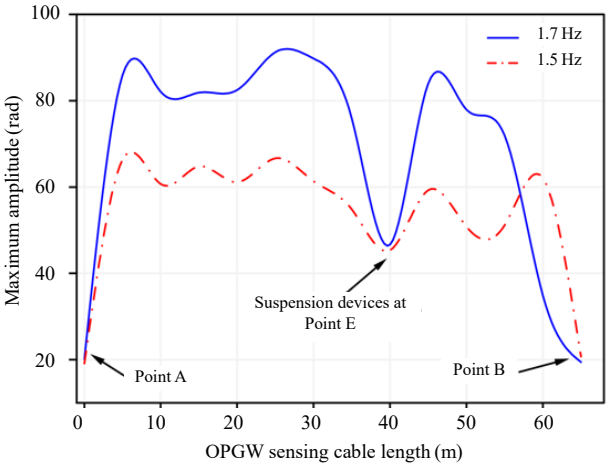


Fig. 12 Comparison of the galloping amplitude at two excitation frequencies.

## 4. Conclusions

We have presented and investigated a distributed online fiber sensing system based on the Φ-OTDR enhanced by the chirped FBG array for overhead transmission lines. The DVS can measure the imposed vibration frequency and amplitude changes along the testing OPGW cable under experimental simulation conditions. Vibration information along

the cable can be collected by adding special sensing fiber containing FBG array. Despite the presence of fiber residual length, the vibration state of small amplitude with several millimeters at high frequency of tens of Hz and the large galloping state with the maximum range of swing to one meter at low frequency of several Hz can be recognized. For the first time, we verify the standing wave motion shape of the OPGW cable through the fiber sensing technology. The experimental results are consistent with the theoretical expectations. The findings are valuable for model establishment and theoretical verification of mechanical structure parameters Through the analysis of experimental data, further improving the spatial resolution and reducing the low-frequency noise of the Φ-OTDR demodulation system are very meaningful to field engineering applications. According to technological trends, by merging the state-of-the-art Φ-OTDR and FBG technology, the DVS can obtain a better signal detection capability. The monitoring of galloping shape and characteristic frequency can predict the trend of destructive vibration behavior and avoid the occurrence of cable breaking and tower toppling accidents, especially the construction and application of ultra-high voltage power grid under severe weather conditions in southern and western China. The proposed system can improve the safety management level of structural health monitoring for overhead transmission lines in smart grid and has a broad application prospect.

## Acknowledgment

This research is supported by the National Natural Science Foundation of China (Grant Nos. 61775173, 61975157, and 52071245) and the Science and Technology Project of State Grid Corporation of China (Research on the basic technology of the next generation intelligent optical cable based on grating array fiber sensor, Grant No. 5442XX190009).

Our acknowledgments go to Eng. Ke Song and Eng. Xin Xiong from Wuhan FLOES Co., Ltd. For their precious help with the technical support of the hardware and software. The authors would also like to acknowledge Dr. Xi Chen and Dr. Yandong Pang in the National Engineering Laboratory for Fiber Optic Sensing Technology for their valuable discussions on paper writing.



## References

[1] J. Jones, M. Ostendorf, and G. Gela, “Fiber optic cables in overhead transmission corridors: a state-of-the-art review,” J.A. Jones Power Delivery, Inc., Haslet, TX, Tech. Rep. TR-108959, Nov. 1997.

[2] J. Wang, “Overhead transmission line vibration and galloping,” in *2008 International Conference on High Voltage Engineering and Application*, Chongqing, China, December, 2008, pp. 120–123.

[3] L. Tian, X. Zhang, and X. Fu, “Fragility analysis of a long-span transmission tower-line system under wind loads,” *Advances in Structural Engineering*, 2020, 23(10): 2110–2120.

[4] S. Wang, X. Jiang, and C. Sun, “Study status of conductor galloping on transmission line,” *High Voltage Engineering*, 2005, 31(10): 11–14.

[5] K. Xie, C. Zhang, Q. Li, W. L. Wu, and Y. Q. Ni, “Tracking galloping profile of transmission lines using wireless inertial measurement units,” *Journal of Computer and Communications*, 2015, 3(05): 57179.

[6] K. J. Zhu, B. Liu, H. J. Niu, and J. H. Li, “Statistical analysis and research on galloping characteristics and damage for iced conductors of transmission lines in China,” in *2010 International Conference on Power System Technology*, Zhejiang, China, 2010, pp. 1–5.

[7] X. Fu, H. N. Li, G. Li, Z. Q. Dong, and M. Zhao, “Failure analysis of a transmission line considering the joint probability distribution of wind speed and rain intensity,” *Engineering Structures*, 2021, 233: 111913.

[8] J. M. Lopez-Higuera, L. R. Cobo, A. Q. Incera, and A. Cobo, “Fiber optic sensors in structural health monitoring,” *Journal of Lightwave Technology*, 2011,

29(4): 587–608.

[9] Q. Huang, C. Zhang, Q. Liu, Y. Ning, and Y. Cao, "New type of fiber optic sensor network for smart grid interface of transmission system," in *IEEE PES General Meeting*, Minneapolis, USA, 2010, pp. 1–5.

[10] L. Bjerkan, "Application of fiber-optic Bragg grating sensors in monitoring environmental loads of overhead power transmission lines," *Applied Optics*, 2000, 39(4): 554–560.

[11] J. Luo, Y. Hao, Q. Ye, Y. Hao, and L. Li, "Development of optical fiber sensors based on Brillouin scattering and FBG for on-line monitoring in overhead transmission lines," *Journal of Lightwave Technology*, 2013, 31(10): 1559–1565.

[12] Z. Xue, Q. Huang, C. Zhang, Y. Cao, and R. Zhang, "Icing monitoring system based on Fiber Bragg Grating sensor for overhead transmission lines," in *2013 IEEE International Conference on Smart Instrumentation, Measurement and Applications (ICSIMA)*, Kuala Lumpur, Malaysia, 2013, pp. 1–4.

[13] Q. Chai, Y. Luo, J. Ren, J. Zhang, J. Yang, L. Yuan, *et al.*, "Review on fiber-optic sensing in health monitoring of power grids," *Optical Engineering*, 2019, 58(7): 072007.

[14] Z. Li, Y. Tong, X. Fu, J. Wang, Q. Guo, H. Yu, *et al.*, "Simultaneous distributed static and dynamic sensing based on ultra-short fiber Bragg gratings," *Optics Express*, 2018, 26(13): 17437–17446.

[15] C. Zhou, Y. Pang, L. Qian, X. Chen, Q. Xu, C. Zhao, *et al.*, "Demodulation of a hydroacoustic sensor array of fiber interferometers based on ultra-weak fiber Bragg grating reflectors using a self-referencing signal," *Journal of Lightwave Technology*, 2018, 37(11): 2568–2576.

[16] J. Jiang, J. Xiong, Z. Wang, Z. Wang, Z. Qiu, C. Liu, *et al.*, "Quasi-distributed fiber-optic acoustic sensing with MIMO technology," *IEEE Internet of Things Journal*, 2021, 8(20): 15284–15291.

[17] M. Wu, X. Fan, Q. Liu, and Z. He, "Highly sensitive quasi-distributed fiber-optic acoustic sensing system by interrogating a weak reflector array," *Optics Letters*, 2018, 43(15): 3594–3597.

[18] T. Liu, H. Li, T. He, C. Fan, Z. Yan, D. Liu, *et al.*, "Ultra-high resolution strain sensor network assisted with an LS-SVM based hysteresis model," *Opto-Electronic Advances*, 2021, 4(5): 200037-1–200037-11.

[19] P. Jousset, T. Reinsch, T. Ryberg, H. Blanck, A. Clarke, R. Aghayev, *et al.*, "Dynamic strain determination using fibre-optic cables allows imaging of seismological and structural features," *Nature Communications*, 2018, 9(1): 1–11.

[20] J. B. Ajo-Franklin, S. Dou, N. J. Lindsey, I. Monga, C. Tracy, M. Robertson, *et al.*, "Distributed acoustic sensing using dark fiber for near-surface characterization and broadband seismic event detection," *Scientific Reports*, 2019, 9(1): 1–14.

[21] G. H. Liang, P. P. Niu, J. Jiang, S. Wang, Y. Wang, J. Xia, *et al.*, "Heterogeneous- frequency-dual-pulse chain and weak FBG array for quasi-distributed acoustic sensing with improved response bandwidth," *Applied Optics*, 2021, 60(25): 7740–7744.

[22] C. Li, J. Tang, C. Cheng, L. Cai, H. Guo, and M. Yang, "Simultaneously distributed temperature and dynamic strain sensing based on a hybrid ultra-weak fiber grating array," *Optics Express*, 2020, 28(23): 34309–34319.

[23] J. P. Jiang, W. B. Gan, Y. Hu, S. Li, J. Deng, L. N. Yue, *et al.*, "Real-time monitoring method for unauthorized working activities above the subway tunnel based on ultra-weak fiber Bragg grating vibration sensing array," *Measurement*, 2021, 182: 109744.

[24] Z. Wang, L. Zhang, S. Wang, N. Xue, F. Peng, M. Fan, *et al.*, "Coherent Φ-OTDR based on I/Q demodulation and homodyne detection," *Optics Express*, 2016, 24(2): 853–858.

[25] Y. Muanenda, "Recent advances in distributed acoustic sensing based on phase-sensitive optical time domain reflectometry," *Journal of Sensors*, 2018, (23): 1–16.

[26] Y. Rao, Z. Wang, H. Wu, Z. Ran, and B. Han, "Recent advances in phase-sensitive optical time domain reflectometry (Φ-OTDR)," *Photonic Sensors*, 2021, 11(1): 1–30.

[27] C. Wang, Y. Shang, X. H. Liu, C. Wang, H. H. Yu, D. S. Jiang, *et al.*, "Distributed OTDR-interferometric sensing network with identical ultra-weak fiber Bragg gratings," *Optics Express*, 2015, 23(22): 29038–29046.

[28] H. M. Irvine and T. K. Caughey, "The linear theory of free vibrations of a suspended cable," *Proceedings of the Royal Society of London. A. Mathematical and Physical Sciences*, 1974, 341(1626): 299–315.

[29] Optical Fiber Composite Overhead Ground Wires. Chinese Standard DL/T 832-2016.

[30] J. Gao, "*Weak signal detection*," Beijing: Tsinghua University Press, 2004: 100–128.